View metadata, citation and similar papers at core.ac.uk
brought to you by CORE
provided by Directory of Open Access Journals

Journal of Applied Fluid Mechanics , Vol. 8, No. 4, pp. 931-941, 2015.
Available online at www.jafmonline.net, ISSN 1735-3572, EISSN 1735-3645.
DOI: 10.18869/acadpub.jafm.67.223.22865

Buoyancy Effects on Unsteady MHD Flow of a Reactive Third-Grade Fluid with Asymmetric Convective Cooling

T. Chinyoka[1,2†] and O.D. Makinde[3]

[1] *Center for Research in Computational and Applied Mechanics, University of Cape Town, Rondebosch 7701, South Africa*
[2] *Department of Chemical Engineering, University of California Santa Barbara, CA 93106-5080 USA*
[3] *Faculty of Military Science, Stellenbosch University, Private Bag X2, Saldanha 7395, South Africa*

† *Corresponding Author Email*: *tchinyok@vt.edu*

(Received April, 1 2014; accepted August, 9 2014)

ABSTRACT

This article examines the combined effects of buoyancy force and asymmetrical convective cooling on unsteady MHD channel flow and heat transfer characteristics of an incompressible, reactive, variable viscosity and electrically conducting third grade fluid. The chemical kinetics in the flow system is exothermic and the asymmetric convective heat transfers at the channel walls follow the Newton's law of cooling. The coupled nonlinear partial differential equations governing the problem are derived and solved numerically using a semi-implicit finite difference scheme. Graphical results are presented and physical aspects of the problem are discussed with respect to various parameters embedded in the system.

Keywords: Buoyancy effect; Unsteady reactive flow; Asymmetrical convective cooling; Magneto-hydrodynamics (MHD); Third grade fluid; Variable viscosity; Finite difference method.

1. INTRODUCTION

Most industrial processes utilize or are affected by reactive fluid flow of Newtonian or non-Newtonian fluid. Examples are abound in the industrial scale polymer and petroleum processing applications (Chinyoka and Makinde 2010). Unlike with the Navier-Stokes equations, no single constitutive equation can model the rheological properties of the collective of non-Newtonian fluids. A number of models have been developed to capture non-Newtonian behavior, see for example (Fosdick and Rajagopal 1980; Makinde 2007). Among these models is the class of third-grade fluids on which this article will be focused.

Magnetohydrodynamic (MHD) processes as well as associated heat transfer processes of non-Newtonian fluids are similarly of great interest in industrial scale applications, say to power engineering, mechanical engineering, nuclear engineering, geophysical fluid dynamics, astrophysical fluid dynamics, etc. (Shercliff 1965). The pioneering work of Hartmann (Hartmann 1937) is considered to be the origin of MHD flow in channels. The main characteristics of MHD flow are based on the observation that the magnetic field enhances the fluid viscosity and thereby offers increased resistance to flow. Several investigations, see for example (Branover 1978) and the references therein, have looked into the effects of applied magnetic fields on channel flow under various conditions. Makinde and Chinyoka (Makinde and Chinyoka 2010; Makinde and Chinyoka 2011; Chinyoka and Makinde 2011) analyzed the transient heat transfer to hydromagnetic channel flow with, among other effects, radiative heat and convective cooling. The effect of magnetic field on boundary layer flow past a vertical plate embedded in a porous medium under convective boundary conditions has been investigated by Makinde and Aziz (Makinde and Aziz 2010).

When the flow is subject to gravitational forces and density variations, say, due to temperature changes, buoyancy effects become important. The buoyancy effects on boundary layer flow

past a vertical plate was first presented by Ostrach (Ostrach 1953). Thereafter, a number of articles have since appeared on this topic with respect to channel flow, see for example the book by Gebhart et al. (Gebhart and Pera 1971). Makinde and Olanrewaju (Makinde and Olanrewaju 2010) studied the buoyancy effects on thermal boundary layers over vertical plates under convective surface boundary conditions. A lot of attention has been devoted to the steady channel flows of non-Newtonian fluids induced by the action of axial pressure gradient in the presence of magnetic fields. Similar attention has also been devoted to thin film flows over moving or stretching surfaces under various conditions, (Prasad, Vajravelu, and Sujatha 2013; Prasad, Vajravelu, Datti, and Raju 2013; Reddy, Raju, and Varma 2013; Loganathan and Stepha 2013; Shit and Majee 2014). Much less effort has been devoted to examining time-dependent flow of similar non-Newtonian fluid flow problems and as far as we are aware, no study appears to have considered the combined effects of buoyancy forces, imposed magnetic field and convective heat exchange at the channel surface on the reactive flow, which is the focus of this investigation.

The objective of the present work is to study unsteady MHD flow of a reactive, variable viscosity, incompressible and third-grade fluid in a vertical channel under asymmetric convective cooling conditions. The MHD effects result from the assumption that the fluid is electrically conducting and that a uniform transverse magnetic field is applied on the flow field. The mathematical formulation of the problem is established in sections two. In section three the semi-implicit finite difference technique is implemented for the solution process. Both numerical and graphical results are presented and discussed quantitatively with respect to various parameters embedded in the system in section four.

2. MATHEMATICAL MODEL

Consider the transient flow of an incompressible electrically conducting, variable viscosity, reactive third grade fluid placed inside a vertical channel induced by the action of applied axial pressure gradient. It is assumed that the flow is subjected to the influence of an externally applied homogeneous magnetic field as shown in Fig.1. The fluid has small electrical conductivity and the electromagnetic force produced is also very small. The channel walls are subjected to unequal convective heat exchange with the ambient. The $\bar{x}$-axis is taken along

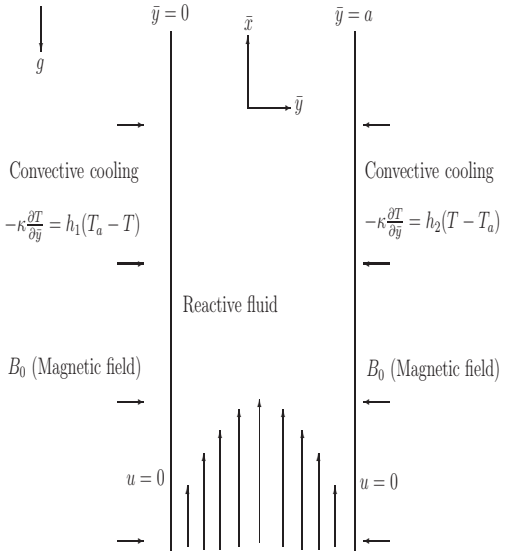

Fig. 1. Geometry of the problem.

the channel and the $\bar{y}$-axis is taken normal to it. The density variation due to buoyancy effects is taken into account in the momentum equation (Boussinesq approximation). Following (Fosdick and Rajagopal 1980; Makinde 2007), and neglecting the reacting viscous fluid consumption, the governing equations for the momentum and heat balance can be written as;

$$\rho\frac{\partial u}{\partial \bar{t}}=-\frac{\partial \bar{P}}{\partial \bar{x}}+\frac{\partial}{\partial \bar{y}}\left[\bar{\mu}(T)\frac{\partial u}{\partial \bar{y}}\right]+\alpha_1\frac{\partial^3 u}{\partial \bar{y}^2\partial \bar{t}}+ 6\beta_3\frac{\partial^2 u}{\partial \bar{y}^2}\left(\frac{\partial u}{\partial \bar{y}}\right)^2-\sigma B_0^2 u+g\beta^*(T-T_0), \quad (1)$$

with the following initial and boundary conditions:

$$u(\bar{y},0)=0,\ T(\bar{y},0)=T_0, \quad (2)$$

$$u(0,\bar{t})=0,\ -k\frac{\partial T}{\partial \bar{y}}(0,\bar{t})=h_1[T_a-T(0,\bar{t})], \quad (3)$$

$$u(a,\bar{t})=0,\ -k\frac{\partial T}{\partial \bar{y}}(a,\bar{t})=h_2[T(a,\bar{t})-T_a], \quad (4)$$

where the additional chemical kinetics term in energy balance equation is due to (Makinde 2007). Here T is the absolute temperature, σ is the fluid electrical conductivity, $B_0(=\mu_e H_0)$ the electromagnetic induction, μ_e is the magnetic permeability, H_0 is the intensity of the magnetic field, ρ is the density, β^* is the volumetric expansion coefficient, g is the gravitational acceleration, c_p specific heat at constant pressure, $\bar{t}$

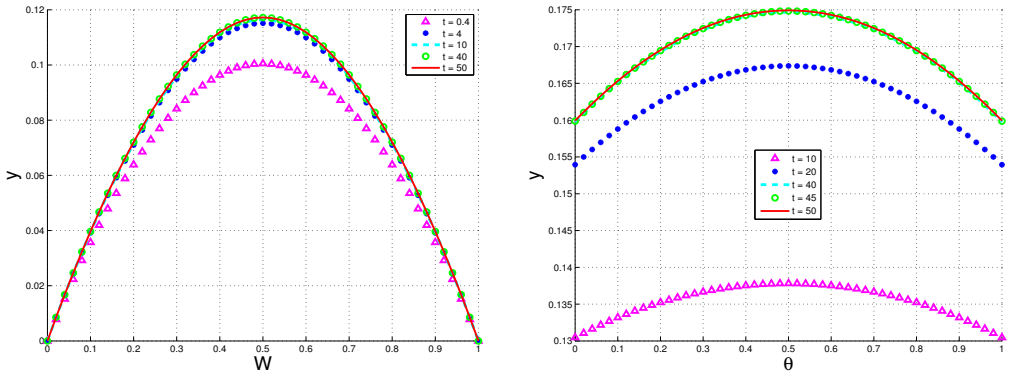

Fig. 2. Transient and steady state velocity and temperature profiles.

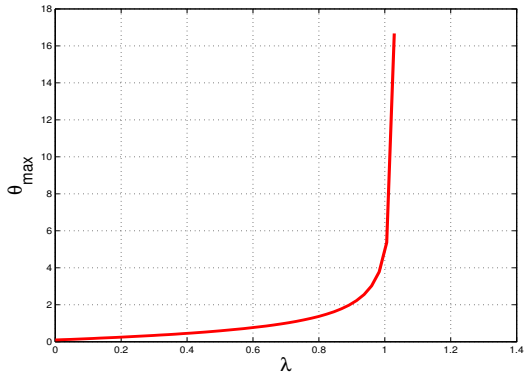

Fig. 3. Blow up of fluid temperature for large λ at time $t = 4$.

is the time, h_1 is the heat transfer coefficient at the left hand side plate, h_2 is the heat transfer coefficient at the right hand side plate, T_0 the fluid initial temperature, T_a is the ambient temperature, k the thermal conductivity of the material, Q the heat of reaction, A is the rate constant, E is the activation energy, R is the universal gas constant, C_0 is the initial concentration of the reactant species, a is the channel width, l is the Planck's number, K is the Boltzmann's constant, ν is the vibration frequency, α_1 and β_3 are the material coefficients, $\bar{P}$ is the modified pressure, m is the numerical exponent such that $m \in \{-2, 0, 0.5\}$, where the three values represent numerical exponents for Sensitised, Arrhenius and Bimolecular kinetics respectively (see (Chinyoka and Makinde 2010; Makinde 2007)). The temperature dependant viscosity ($\bar{\mu}$) can be expressed as

$$\bar{\mu}(T) = \mu_0 e^{-b(T-T_0)}, \tag{5}$$

where b is a viscosity variation parameter and μ_0 is the initial fluid dynamic viscosity at temperature T_0. We introduce the following dimensionless variables into Eqs. (1) - (5);

$$y = \frac{\bar{y}}{a}, x = \frac{\bar{x}}{a}, t = \frac{\bar{t}\mu_0}{\rho a^2}, W = \frac{u\rho a}{\mu_0}, \mu = \frac{\bar{\mu}}{\mu_0},$$
$$\alpha = \frac{bRT_0^2}{E}, \theta = \frac{E(T-T_0)}{RT_0^2}, \theta_a = \frac{E(T_a-T_0)}{RT_0^2},$$
$$\gamma = \frac{\beta_3\mu_0}{\rho^2 a^4}, \delta = \frac{\alpha_1}{\rho a^2}, \mathrm{Bi}_1 = \frac{h_1 a}{k}, \mathrm{Bi}_2 = \frac{h_2 a}{k},$$
$$\mathrm{Pr} = \frac{\mu_0 c_p}{k}, \lambda = \left(\frac{KT_0}{\nu l}\right)^m \frac{QEAa^2C_0 e^{-\frac{E}{RT}}}{T_0^2 Rk},$$
$$\varepsilon = \frac{RT_0}{E}, P = \frac{\bar{P}\rho a^2}{\mu_0^2}, G = -\frac{\partial \bar{P}}{\partial x},$$

$$\mathrm{Ha}^2 = \frac{\sigma B_0^2 a^2}{\mu_0}, \mathrm{Gr} = \frac{g\beta^* RT_0^2 a^3 \rho^2}{E\mu_0^2},$$
$$\Omega = \left(\frac{\nu l}{KT_0}\right)^m \frac{\mu_0^3 e^{\frac{E}{RT}}}{\rho^2 QAa^4 C_0}, \tag{6}$$

and obtain the following dimensionless governing equations;

$$\frac{\partial W}{\partial t} = G - \mathrm{Ha}^2 W + e^{-\alpha\theta}\frac{\partial^2 W}{\partial y^2} + \mathrm{Gr}\theta + \delta\frac{\partial^3 W}{\partial y^2 \partial t} - \alpha e^{-\alpha\theta}\frac{\partial\theta}{\partial y}\frac{\partial W}{\partial y} + 6\gamma\frac{\partial^2 W}{\partial y^2}\left(\frac{\partial W}{\partial y}\right)^2, \tag{7}$$

$$\mathrm{Pr}\frac{\partial\theta}{\partial t} = \frac{\partial^2\theta}{\partial y^2} + \lambda\left\{(1+\varepsilon\theta)^m \exp\left(\frac{\theta}{1+\varepsilon\theta}\right) + \Omega\left[\mathrm{Ha}^2 W^2 + \left(\frac{\partial W}{\partial y}\right)^2\left(e^{-\alpha\theta} + 2\gamma\left(\frac{\partial W}{\partial y}\right)^2\right)\right]\right\}, \tag{8}$$

$$W(y,0)=0,\ \theta(y,0)=0, \tag{9}$$

$$W(0,t)=0, \frac{\partial\theta}{\partial y}(0,t)=-\mathrm{Bi}_1\left[\theta_a-\theta(0,t)\right], \tag{10}$$

$$W(1,t)=0, \frac{\partial\theta}{\partial y}(1,t)=-\mathrm{Bi}_2\left[\theta(1,t)-\theta_a\right], \tag{11}$$

where $\lambda, \mathrm{Pr}, \mathrm{Bi}, \varepsilon, \delta, \gamma, G, \mathrm{Gr}, \alpha, \Omega, \theta_a, \mathrm{Ha}$ represent the Frank-Kamenetskii parameter, Prandtl number, Biot number, activation energy parameter, material parameter, non-Newtonian parameter, pressure gradient parameter, Buoyancy paramter, variable viscosity parameter, viscous heating parameter, the ambient temperature parameter and Hartmann number, respectively. The other dimensionless quantities of interest are the skin friction (C_f) and the wall heat transfer rate (Nu) given as

$$C_f=-\frac{dW}{dy}(1,t), \quad Nu=-\frac{d\theta}{dy}(1,t). \tag{12}$$

In the following section, the Eqs. (7) - (12) are solved numerically using a semi-implicit finite difference scheme.

3. Numerical Solution

Our numerical algorithm is based on the semi-implicit finite difference scheme given in Chinyoka *et al.* (Chinyoka, Renardy, Renardy, and Khismatullin 2005; Chinyoka 2008; Chinyoka 2011; Ireka and Chinyoka 2013; Chinyoka, Goqo, and Olajuwon 2013) for the isothermal viscoelastic case. As in Chinyoka (Chinyoka 2008), we extend the algorithm to the temperature equation and take the implicit terms at the intermediate time level $(N+\xi)$ where $0 \leq \xi \leq 1$. The algorithm employed in Chinyoka (Chinyoka 2008) uses $\xi = 1/2$, we will however follow the formulation in Chinyoka *et al.* (Chinyoka, Renardy, Renardy, and Khismatullin 2005) and thus take $\xi = 1$ in this article so that we can use larger time steps.

4. Results and Discussion

Unless otherwise stated, we employ the parameter values:

$G=1,\ \mathrm{Gr}=0.1,\ \mathrm{Pr}=10,\ \theta_a=0.1,\ \delta=0.1, \lambda=0.1,\ \mathrm{Bi}_1=1,\ \mathrm{Bi}_2=1\ m=0.5,\ \varepsilon=0.1, \alpha=0.1, \Omega=0.1, \gamma=0.1, \mathrm{Ha}=1,\ \Delta y=0.02, \Delta t=0.001$ and $t=20$.

These will be the default values in this work and hence in any graph where any of these parameters is not explicitly mentioned, it will be understood that such parameters take on the default values.

4.1 Transient and Steady Flow Profiles

We display the transient solutions in Fig. 2. The figures show a transient increase in both fluid velocity and temperature until a steady state is reached.

4.11 Blow up of solutions

We need to point out early on that depending on certain parameter values in the problem, the steady temperature and velocity profiles, such as those shown in Fig. 2, may not be attainable. In particular, the reaction parameter λ will need to be carefully controlled as "large" values can easily lead to blow up of solutions as illustrated in Fig. 3. As shown in Fig. 3, larger values of λ would lead to finite time temperature blow up since the terms associated with λ are strong heat sources.

4.12 Parameter dependance of solutions

The response of the velocity and temperature to varying values of the Hartmann number (Ha) is illustrated in Fig. 4. An increase in the parameter Ha leads to corresponding increases in damping magnetic properties of the fluid. These forces result in increased resistance to flow and thus explain the reduction in fluid velocity with increasing Hartmann number, see Fig. 4. The reduced velocity in turn decreases the viscous heating source terms in the temperature equation and hence correspondingly decreases the fluid temperature as shown in Fig. 4. The response of the velocity and temperature to varying values of the non-Newtonian parameter (γ) is illustrated in Fig. 5. An increase in the parameter γ leads to corresponding increases in those non-Newtonian properties of the fluid, say (visco)elasticity, that would result in increased resistance to flow and thus explain the slight reduction in fluid velocity with increasing non-Newtonian character as measured by the parameter γ, see Fig. 5. The reduced velocity in turn decreases the viscous heating source terms in the temperature equation and hence correspondingly decreases the fluid temperature as shown in Fig. 5. Since however the parameter γ only enters the temperature equation implicitly through the velocity field, the effects of γ on the fluid temperature are not as noticeable as on the fluid velocity. The influence of the variable viscosity parameter on the velocity and temperature profiles is shown in Fig. 6. Increasing the parameter α reduces the fluid

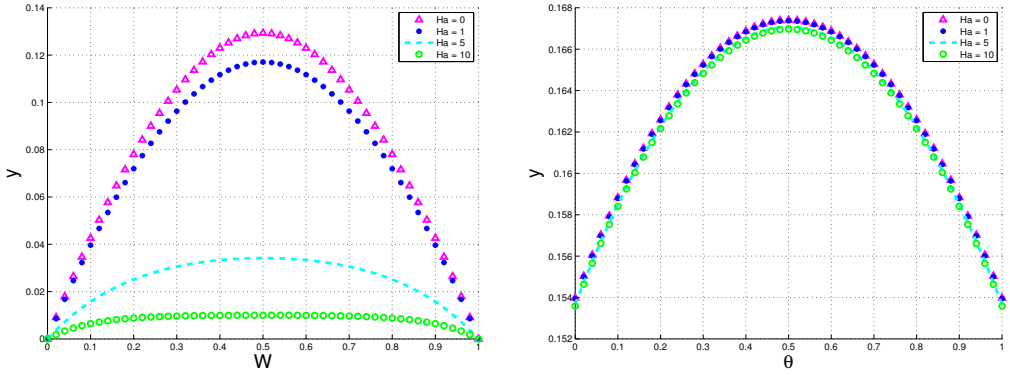

Fig. 4. Effects of Hartmann number (Ha) **on velocity and temperature.**

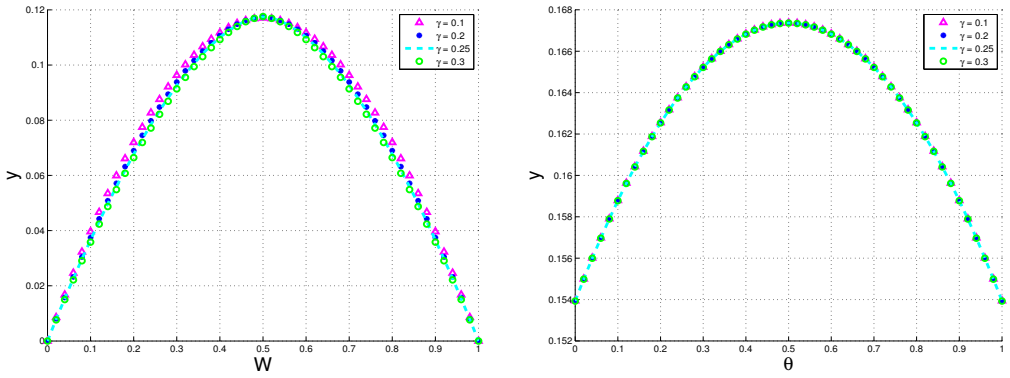

Fig. 5. Effects of non-Newtonian parameter (γ) on velocity and temperature.

viscosity and hence correspondingly diminishes the fluid's resistance to flow. This necessarily leads to increased fluid velocity as illustrated in Fig. 6. The increased velocity in turn increases the viscous heating source terms in the temperature equation and hence correspondingly increases the fluid temperature as shown in Fig. 6. As with the non-Newtonian parameter, the viscous effects are more pronounced in the velocity equation than in the temperature equation and this explains why the effects of α on the fluid temperature are not as noticeable as in the fluid velocity. The effects of the chemical kinetics exponent m on the velocity and temperature profiles is shown in Fig. 7. Figure 7 shows that the internal heat generated in the fluid during a bimolecular type of exothermic chemical reaction $(m = 0.5)$ is higher than that generated either under the Arrhenius $(m = 0)$ or Sensitised $(m = -2)$ reaction types. This is so since an increase in the parameter m leads to corresponding increases in the strengths of the chemical reaction source terms in the temperature equation. This leads to increased fluid temperatures as shown in Fig. 7. The increased temperature in turn leads to a reduction in fluid viscosity and hence indirectly to increased fluid velocity as illustrated in Fig. 7. Since however the parameter m only enters the velocity equation implicitly through the temperature/viscosity coupling, the effects of m on the fluid velocity at best look marginal and are not as pronounced as on the fluid temperature. The effects of the activation energy parameter ε on the velocity and temperature profiles is shown in Fig. 8. The parameter ε plays a more-or-less similar role (both Mathematically and physically) to the parameter m described in the earlier Fig. 7 and hence its effects are similarly explained. The graphs of Fig. 8 correspond to the case of Bimolecular reactions $(m = 0.5)$. It should however be noted that in the cases of Sensitized and Arrhenius reactions (in which $m \leq 0$) both temperature and velocity are expected to decrease with increasing ε, see Fig. 9.

This is due to the fact that the function:

$$(1+\varepsilon\theta)^m \exp\left(\frac{\theta}{1+\varepsilon\theta}\right), \qquad m \leq 0,] \qquad (13)$$

decreases as ε increases. Since this function represents source terms in the temperature equation, the fluid temperature expectedly decreases with increasing ε, so that the maximum

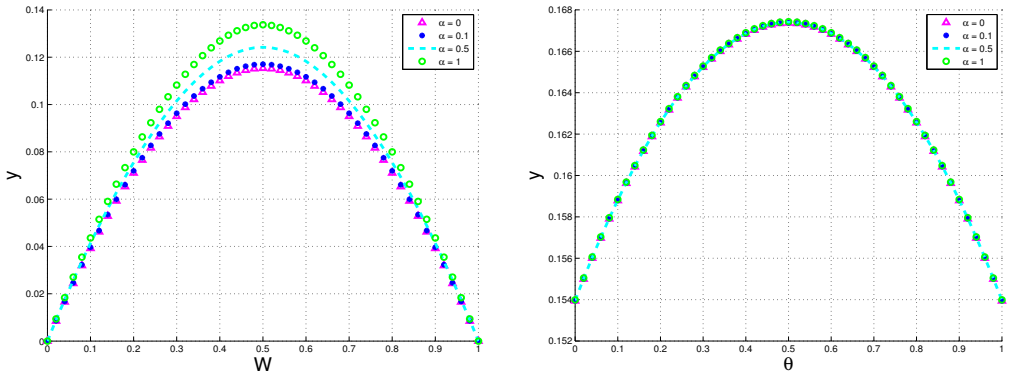

Fig. 6. Effects of variable viscosity parameter (α) on velocity and temperature.

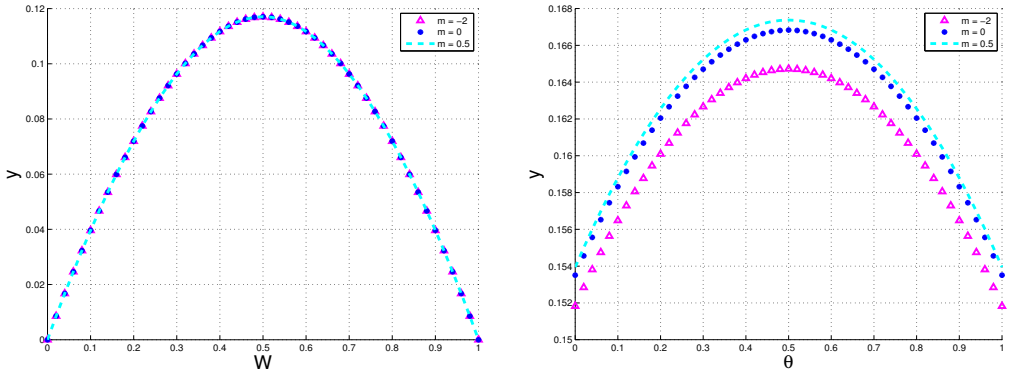

Fig. 7. Effects of parameter (m) on velocity and temperature.

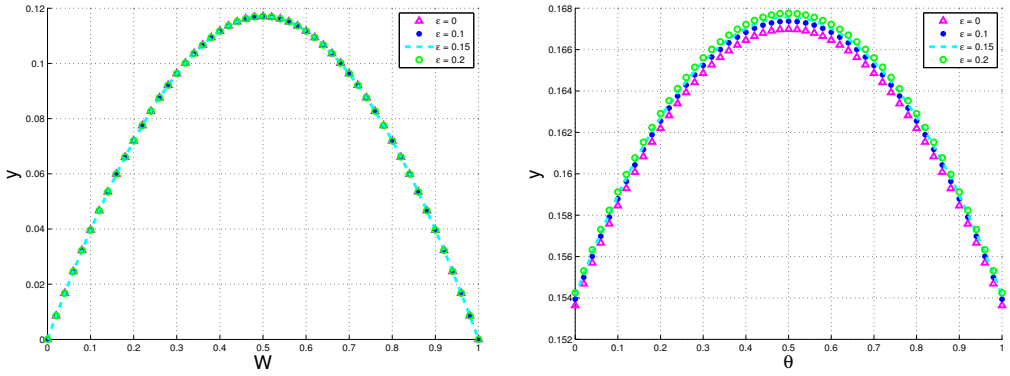

Fig. 8. Effects of activation energy parameter (ε) on velocity and temperature.

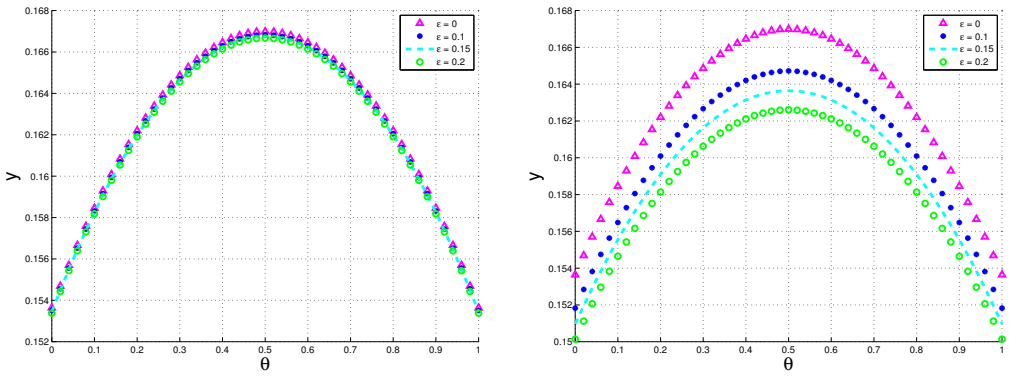

(a) $m = 0$ (b) $m = -2$

Fig. 9. Effects of activation energy parameter (ε) on temperature.

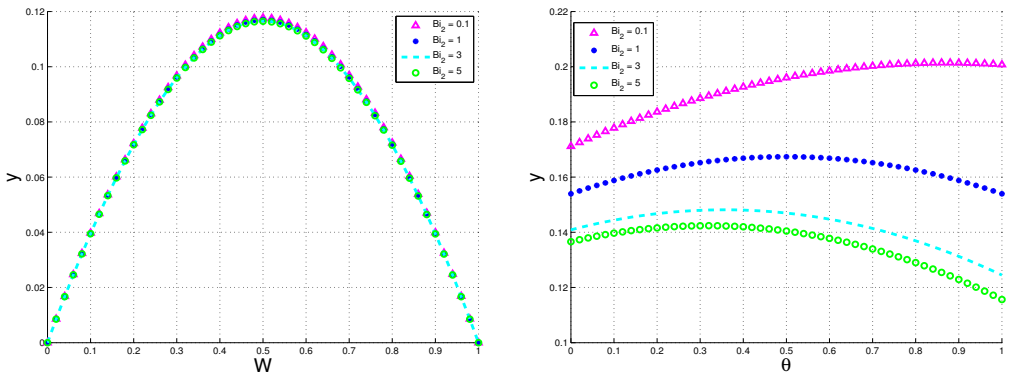

Fig. 10. Effects of the Biot number (Bi_2) on velocity and temperature.

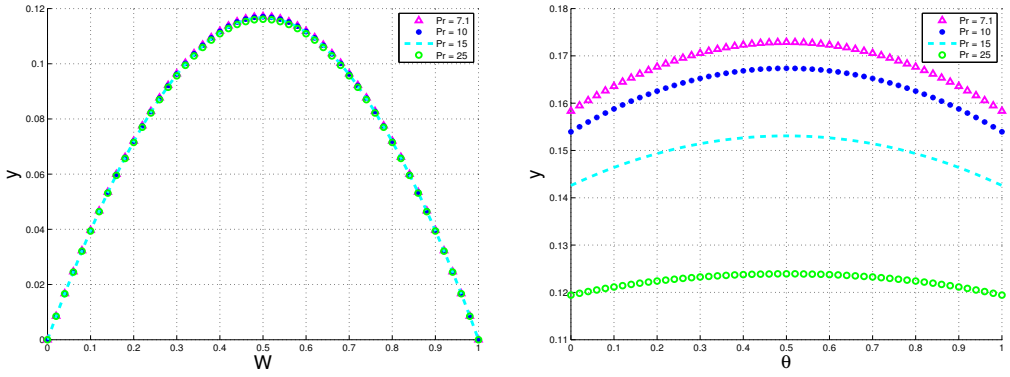

Fig. 11. Effects of the Prandtl number (Pr) on velocity and temperature.

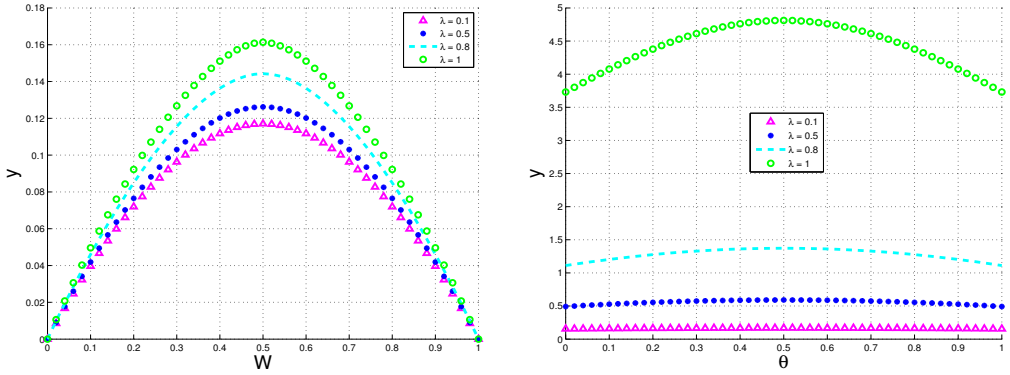

Fig. 12. Effects of the reaction parameter (λ) on velocity and temperature.

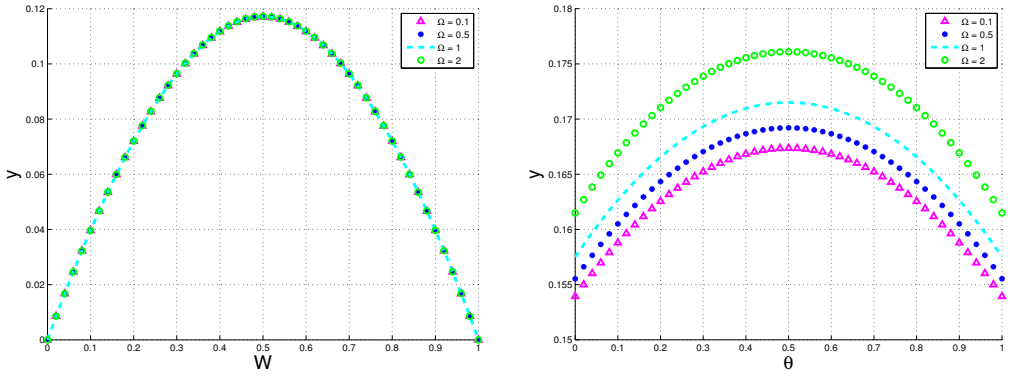

Fig. 13. Effects of the viscous heating parameter (Ω) on velocity and temperature.

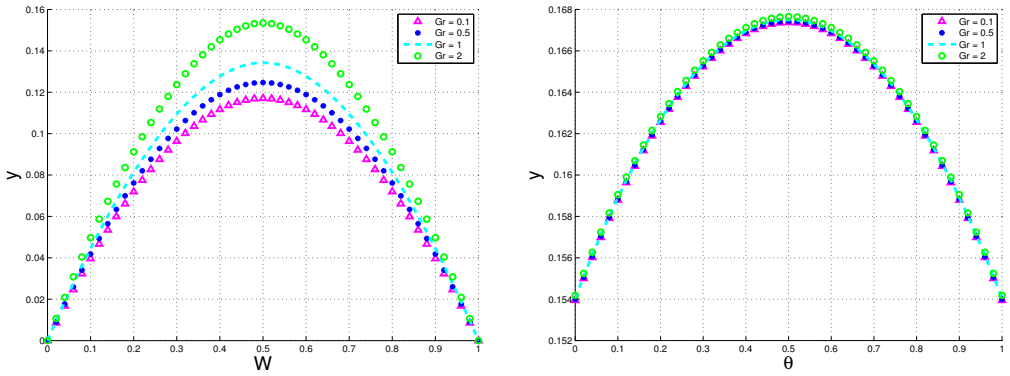

Fig. 14. Effects of the buoyancy parameter (Gr) on velocity and temperature.

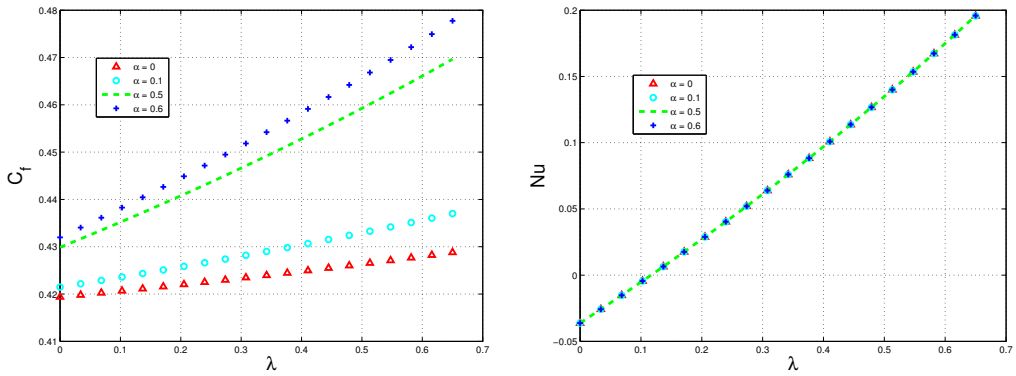

Fig. 15. Variation of C_f and Nu with λ and α.

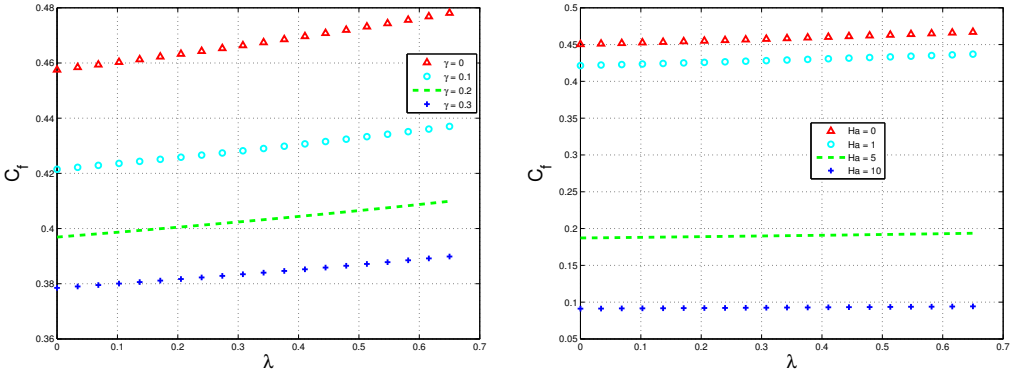

Fig. 16. Variation of wall shear stress with λ, γ and Ha**.**

temperature is recorded for $\varepsilon = 0$ as shown in Fig. 9. The effects of the Biot number Bi_2 on the velocity and temperature profiles is illustrated in Fig. 10. As seen from the temperature boundary condition, Eq. (11), higher Biot numbers mean correspondingly higher degrees of convective cooling at the channel walls and hence lead to lower temperatures at the channel walls and hence also in the bulk fluid. The overall temperature profiles thus decrease with increasing Biot number as the bulk fluid continually adjusts to the lower wall temperatures. The reduced temperatures correspondingly decrease the fluid viscosity and hence also marginally decreases the fluid velocity through the viscosity coupling. As noted earlier, such a coupling depends on other parameters as well (say α) does not necessarily result in drastic changes in velocity profiles even though the temperature profiles show well pronounced changes, see Fig. 10. The effects of the Prandtl number Pr on the velocity and temperature profiles is illustrated in Fig. 11. Larger values of the Prandtl number correspondingly decrease the strength of the source terms in the temperature equation and hence in turn reduces the overall fluid temperature as clearly illustrated in Fig. 11. As pointed out earlier, the reduced temperature results in decreased fluid viscosity and hence reduced fluid velocity, see Fig. 11. The effects of the reaction parameter λ on the velocity and temperature profiles is illustrated in Fig. 12 respectively. The reaction parameter λ plays a roughly opposite role to the Prandtl number just described. Increased values of λ lead to significant increases in the reaction and viscous heating source terms and hence significantly increase the fluid temperature as shown in Fig. 12 and also in the blow up figure Fig. 3. The significant temperature rise in response to the increased λ mean that the viscosity coupling to the velocity is no longer weak and hence significant reductions in the viscosity lead to appreciable increases in the fluid velocity. The effects of the viscous heating parameter Ω on the velocity and temperature profiles is illustrated in Fig. 13. The effects of Ω mirror those of λ, albeit on a smaller scale since Ω is not connected to the exponentially increasing reaction source terms but only to the viscous heating terms. The effects of the buoyancy parameter Gr on the velocity and temperature profiles is illustrated in Fig. 14 respectively. An increase in the buoyancy parameter Gr leads to a corresponding increase in the fluid velocity and shown in Fig. 14. This results from the fact that the Buoyancy terms act as source terms in the momentum relation. The increased velocity correspondingly increases the fluid temperature, albeit on a smaller scale, due to reasons already given earlier. The wall shear stress (C_f) and wall heat transfer rate (Nu) dependance on the reaction parameter λ is illustrated in Fig. 15 for varying values of the viscosity variation parameter α. Figure 16 shows the wall shear stress dependance on λ for varying values of the non-Newtonian parameter γ and and also for varying values of the Hartmann number Ha. In general, parameters that decrease (increase) the fluid velocity correspondingly decrease (increase) the wall shear stress respectively. The wall heat transfer dependance on λ for varying values of γ and the wall heat transfer dependance on λ for varying values of Ha are both qualitatively similar to the wall heat transfer rate dependance on λ for varying values of α as shown in Fig. 15. As with the wall shear stress, parameters that decrease (increase) the fluid temperature correspondingly decrease (increase) the wall heat transfer. In fact, since both the parameters α and γ only marginally increase the temperature, their effects on the wall heat transfer are also similarly marginal. All the results for the wall shear stress and the wall heat transfer were obtained at time $t = 5$.

5. CONCLUSION

We computationally investigate the Buoyancy effects on unsteady MHD flow of a reactive third-grade fluid with asymmetric convective cooling. We observe that there is a transient increase in both fluid velocity and temperature with an increase in the Buoyancy, reaction strength, viscous heating and fluid viscosity parameter (which decreases the viscosity). A transient decrease in both fluid velocity and temperature is observed with an increase in the non-Newtonian character and magnetic field strength. The possible finite time blow-up of solutions means that the reaction strength needs to be carefully controlled. We also notice that due to the nature of the coupling of the source terms, the fluid velocity and temperature either both increase or both decrease together. Parameters that increase any such source terms would increase these quantities and similarly those that decrease the source terms correspondingly decrease the flow quantities.

REFERENCES

Branover, H. (1978). *MHD flow in Ducts*. Keter Publ. House Jerusalem Ltd.: Wiley and Israel Univ. Press.

Chinyoka, T. (2008). Computational dynamics of a thermally decomposable viscoelastic lubricant under shear. *Transactions of ASME Journal of Fluids Engineering 130*(12), 121201(1–7).

Chinyoka, T. (2011). Suction-injection control of shear banding in non-isothermal and exothermic channel flow of johnsonsegalman liquids. *Transactions of ASME Journal of Fluids Engineering 133*(7), 071205(1–12).

Chinyoka, T., S. Goqo, and B. Olajuwon (2013). Computational analysis of gravity driven flow of a variable viscosity viscoelastic fluid down an inclined plane. *Computers & Fluids 84*(15), 315–326.

Chinyoka, T. and O. Makinde (2010). Computational dynamics of unsteady flow of a variable viscosity reactive fluid in a porous pipe. *Mechanics Research Communications 37*, 347353.

Chinyoka, T. and O. Makinde (2011). Analysis of transient generalized couette flow of a reactive variable viscosity third-grade liquid with asymmetric convective cooling. *Mathematical and Computer Modelling 54*(1-2), 160174.

Chinyoka, T., Y. Renardy, M. Renardy, and D. Khismatullin (2005). Two-dimensional study of drop deformation under simple shear for oldroyd-b liquids. *Journal of Non-Newtonian Fluid Mechanics 31*, 45–56.

Fosdick, R. and K. Rajagopal (1980). Thermodynamics and stability of fluids of third grade. *Proc. Roy. Soc. London A339*, 351.

Gebhart, B. and L. Pera (1971). The nature of vertical natural convection flows resulting from the combined buoyancy effects of thermal and mass diffusion. *Int. J. Heat Mass Transfer 14*, 2025–2050.

Hartmann, J. (1937). Theory of laminar flow of an electrically conducting liquid in a homogeneous magnetic field, hg-dynamics i. *Math. Fys. Med. 15*, 1–28.

Ireka, I. and T. Chinyoka (2013). Non-isothermal flow of a johnsonsegalman liquid in a lubricated pipe with wall slip. *Journal of Non-Newtonian Fluid Mechanics 192*, 20–28.

Loganathan, P. and N. Stepha (2013). Chemical reaction and mass transfer effects on flow of micropolar fluid past a continuously moving porous plate with variable viscosity. *Journal of Applied Fluid Mechanics 6*(4), 581–588.

Makinde, O. (2007). Thermal stability of a reactive third grade fluid in a cylindrical pipe: An exploitation of hermite-padé approximation technique. *Applied Mathematics and Computation 189*, 690697.

Makinde, O. and T. Chinyoka (2010). Numerical investigation of transient heat transfer to hydromagnetic channel flow with radiative heat and convective cooling. *Communications in Nonlinear Science and Numerical Simulations 15*, 3919–3930.

Makinde, O. and T. Chinyoka (2011). Numerical study of unsteady hydromagnetic generalized couette flow of a reactive third-grade fluid with asymmetric convective cooling. *Computers & Mathematics with Applications 61*(4), 11671179.

Makinde, O. and P. Olanrewaju (2010). Buoyancy effects on thermal boundary layer over a vertical plate with a convective surface boundary condition. *Transaction of ASME Journal of Fluid Engineering 132*, 044502(1–4).

Makinde, O. D. and A. Aziz (2010). Mhd mixed convection from a vertical plate embedded in a porous medium with a convective boundary condition. *International Journal of Thermal Sciences 49*, 1813–1820.

Ostrach, S. (1953). An analysis of laminar free convection flow and heat transfer along a flat plate parallel to the direction of the generating body force. In *NACA Report 1111*.

Prasad, K., K. Vajravelu, P. Datti, and B. Raju (2013). Mhd flow and heat transfer in a power-law liquid film at a porous surface in the presence of thermal radiation. *Journal of Applied Fluid Mechanics 6*(3), 385–395.

Prasad, K., K. Vajravelu, and A. Sujatha (2013). Influence of internal heat generation/absorption, thermal radiation, magnetic field, variable fluid property and viscous dissipation on heat transfer characteristics of a maxwell fluid over a stretching sheet. *Journal of Applied Fluid Mechanics 6*(2), 249–256.

Reddy, T., M. Raju, and S. Varma (2013). Unsteady mhd radiative and chemically reactive free convection flow near a moving vertical plate in porous medium. *Journal of Applied Fluid Mechanics 6*(3), 443–451.

Shercliff, J. (1965). *A Textbook of Magnetohydrodynamics*. London, UK.: Pergoman Press.

Shit, G. and S. Majee (2014). Hydromagnetic flow over an inclined non-linear stretching sheet with variable viscosity in the presence of thermal radiation and chemical reaction. *Journal of Applied Fluid Mechanics 7*(2), 239–247.